Assessment of lime treatment of expansive clays with different mineralogy at low and high temperatures

Hatim Ali and Mostafa Mohamed

Hatim Ali PhD research student, Civil Engineering Department, Faculty of Engineering and Informatics

University of Bradford, Bradford, West Yorkshire, BD7 1DP, UK.

h.f.a.ali@student.bradford.ac.uk

Mostafa Mohamed Senior Lecturer, Civil Engineering Department, Faculty of Engineering and Informatics

University of Bradford, Bradford, West Yorkshire, BD7 1DP, UK.

m.h.a.mohamed@bradford.ac.uk

Corresponding author:

Dr Mostafa Mohamed

Email: M.h.a.mohamed@bradford.ac.uk

Phone: +44(0) 1274 233856

Fax: +44(0) 1274 2341111

Re-submission

26th June 2019

Assessment of lime treatment of expansive clays with different mineralogy at low and high temperatures

H. Ali and M. Mohamed

Abstract: This paper examines the impacts of clay mineralogy on the effectiveness of lime stabilisation at different temperatures. A comprehensive experimental programme was conducted to track down the evolution of lime-clay reactions and their durations through monitoring the evolution of strength gain at predetermined times using the Unconfined Compressive Strength (UCS) test. The study examined clays with different mineralogy compositions comprising Na^+ Bentonite and Ball (Kaolinite) clay. Four different clays were tested including 100% bentonite, 100% Ball clay and two clay mixtures with ratios of 1:1 and 1:3 by mass of bentonite to Ball clay. All clays were treated using a range of lime content up to 25% and cured for a period of time up to 672 h at two different temperatures of 20 and 40^{o}C. The results showed that the continuity of the fast phase (stage 1) of strength gain was dependent on the availability of lime in particular at the higher temperature. Whereas, for the same lime content, the duration of the fast phase and the kinetic of strength gain were significantly related to the clay mineralogy and curing temperature. Except for the initial strength gain at 0 h curing time, the lime-treated Ball clay specimens at 20^{o}C appeared to show no strength gain throughout the curing period that extended up to 672 h. However, when curing occurred at 40^{o}C, the no strength gain stage only lasted for 72 h after which a gradual increase in the strength was observed over the remaining curing period of time. The addition of Bentonite to Ball clay succeeded in kicking off the strength gain after a short period of curing time at both curing temperatures.

Keywords: Lime stabilised clays, clay mineralogy, Unconfined Compressive Strength, Curing temperature, Pozzolanic reaction.

1. Introduction

Natural soils in work-sites are sometimes detrimental to the construction of engineering projects. Problematic soils such as soft and expansive soils are a real source of concern to the long term stability of structures if care is not taken. Expansive soils could generate huge distress due to their volume change in response to a slight change in their water content. On the other hand, soft soils are characterized by their low shear strength and poor workability. In earthwork, replacing these soils is sometimes economically and sustainably unjustifiable in particular if they can be stabilised to improve their behaviour. Several techniques have evolved to enable construction on problematic soils such as reinforcement using fibre and planar layers (see for example; Mohamed 2010; Mirzababaei et al., 2017 and 2018), piled reinforced embankments (see for example; Aqoub et al., 2018) and chemical agent (see for example; Alrubaye et al., 2018; Coudert et al., 2019; Kang et al., 2019; Yaghoubi et al., 2019)

Chemical treatment using e.g. lime and/or cement is an alternative method to seize the volume change of swelling clays. The use of lime as a binding agent is becoming a popular method due to its abundant availability and cost-effectiveness. When mixed with swelling clays, lime enhances the mechanical properties, workability and reduce sensitivity to absorption and release of water. The lime in both states; Hydrated lime $Ca(OH)_2$ and Quick lime CaO, have been used to stabilised swelling clays. Cation exchange, flocculation and agglomeration, and pozzolanic reaction in addition to carbonization are well-reported mechanisms that are in charge of causing changes in the clay characteristics after the addition of the lime in the presence of water. These mechanisms have been subjected to numerous investigations (see for example; Diamond and Kinter, 1965; Rogers and Roff, 1997; Boardman et al., 2001; Puppala et al., 2005; Di Sante et al., 2014; Zhao et al., 2015; Vitale et al., 2016; Vitale et al., 2017; Chemeda et al., 2018; Gao et al., 2018; Di Sante et al., 2019). Precisely, the added lime dissolves partially into calcium ions and hydroxyl ions in the pore water. The calcium ions as divalent cations resort to subrogate the lesser charge cations surrounding the surface of clay particles in a mechanism so-called cation exchange. The surfaces of clay particles inherently carry negative

charges which are balanced by native cations forming a diffuse double layer surrounding each clay particle. The cation exchange leads to a reduction in the thickness of the diffuse double layer, hence the charge on the surface of clay particles is balanced by a smaller number of cations (Strawn et al., 2015). Immediately, neighbouring clay particles become closer and interact with each other leading to the reconfiguration of their positions into flocs and clusters in a so-called flocculation and agglomeration mechanism. In contrast, the release of hydroxyl ions creates an alkaline environment in the pore water. Such an aggressive alkaline environment attacks the surface of clay particle, causing a launch of alumina and silica ions in the pore water. These ions react with the available calcium and hydroxyl ions to form the cementitious compounds in a process called “pozzolanic reaction”. However, a point of controversy remains as to whether these mechanisms take place consecutively or simultaneously (Boardman et al., 2001).

The effect of the aforementioned mechanisms and reactions is tangible through observing the changes that occur in the soil characteristics such as swelling behaviour, plasticity indices, hydraulic conductivity, compaction and strength. The strength of lime-stabilised clays is one of the key parameters required in the engineering design of earthworks. Necessities for assessing the evolution of strength, long-term stability and desirable lime content require the need for not only a practical but also a relatively quick test. Unconfined Compressive Strength (UCS) was reported to satisfactorily suit the requirement to determine the lime content that is desirable to cause an optimum change in the strength properties. A few studies used the UCS tests as a mean to monitor the evolution of lime reaction. Locat et al. (1990) monitored the development of strength gain in four types of sensitive clays that were treated by different lime contents reaching up to 10%. The results showed that the strength gain passed through three distinct phases. The strength gain showed small improvement during the first phase, followed by a significant growth during the intermediate phase before slowing down or even coming to a halt through the final phase. Locat et al. (1990) attributed the behaviour of strength over the final phase to the completion of the pozzolanic reaction. Hashemi

et al. (2018) observed similar three phases for the strength development over a curing period of up to 28 days on sand-bentonite mixtures that were treated by various percentages of quick lime ranging from 3 to 8%. However, both studies did not indicate the role of curing temperature on the evolution of strength gain. Using chemical approaches, Al-Mukhtar et al. (2010a) and Al-Mukhtar et al. (2010b) demonstrated that the rate of pozzolanic reaction at a curing temperature of 50^{o}C was six-fold higher than that observed to occur at a curing temperature of 20^{o}C. This was in agreement with the finding of an experimental investigation that was conducted by De Windt et al. (2014) to evaluate the impact of curing times up to 98 days and two ambient temperatures of 20 and 50^{o}C on lime treated bentonite. The results showed that the ambient temperature of 50^{o}C multiplied the kinetic of pozzolanic reaction by five times compared with that observed at a curing temperature of 20^{o}C.

. The effectiveness of lime stabilization was found to be dependent on many key parameters such as mineralogy composition of clay, lime content, moisture content, mixing time and technique, mellowing time, mellowing temperature, compaction method, dry unit weight, curing temperature and curing time (Bell, 1996; Bozbey and Garaisayev, 2010; Kitazume and Terashi, 2013; Ali and Mohamed, 2017; Ali and Mohamed, 2018; Al-Alwan, 2019; Jahandari et al., 2019). These key parameters require systematic testing and evaluation. In the current study, four clays with different mineralogy compositions, covering a wide range of liquid limit were used. Lime with a range of 5 to 25 % by dry weight was added to clays with different mineralogical compositions to assess its effect on the evolution of strength and the continuity of chemical reactions at 20 and 40^{o}C throughout a curing period that lasted up to 672 h. Earlier results of (Ali and Mohamed, 2018) on lime stabilised bentonite with up to 13% lime showed the occurrence of two distinct stages in the strength gain that are dependent upon lime content and temperature. However, authors did not assess different clays and the continuity of the distinct stages, in particular, the short-term fast strength gain, at higher lime contents and extended period of curing time. Therefore, this paper aims to provide a comprehensive assessment of the kinetic of strength gain in the short- and long-term stages so as to enable deep

120 understanding of the key factors that govern the kinetics of strength gain over time in different soils.
121 Furthermore, the results are coupled with and supported by earlier studies on the microstructure and
122 chemical reactions to strengthen the discussion on the changes in the strength characteristics.

123 ## 2. Methodology

124 ### 2.1. Materials

125 Two different types of clay, namely Bentonite and Ball clays, were used in the current study. The main
126 clay mineral in the Bentonite is the montmorillonite mineral, whereas the kaolinite mineral is the
127 major clay mineral in the Ball clay. All clays were supplied by Potclays Ltd, UK in a powder form. The
128 chemical analysis of both Bentonite and Ball clays are shown in Table 1. Both clays were mixed in
129 different proportions to obtain two additional clay mixtures with a ratio of 1:3 and 1:1 Bentonite to
130 Ball clay by dry mass, as illustrated in Table 2. The Bentonite-Ball clay mixtures were selected to assess
131 the accumulation of calcium on the surface of kaolinite particles which might cause delay of
132 disassociation of alumina and silica ions by preventing the alkaline environment from attacking the
133 surface of kaolinite particles. In this case, Bentonite, which is an active clay, is introduced in the mix
134 as a rival consumer for the calcium to reduce the potential accumulation of calcium. The potential
135 reduction in the accumulation of calcium cations allows the alkaline environment to attack the surface
136 of clay particles to begin the dissolution of alumina and silica and thus, to initiate the formation of
137 cementitious compounds and strength gain in a shorter time. The geotechnical properties of the four
138 used clays in this investigation are illustrated in Table 2. The experimental data for the characterization
139 of clay materials showed that the Liquid Limit (LL) of M1 which is pure Bentonite clay is 320% whereas
140 that of Ball clay is 58%. The other two mixtures that were created by different ratios retained LL of
141 115 and 189% for M3 and M4 respectively. These data demonstrated that the four materials
142 represented a vast range of liquid limit and plasticity index spanning from 320% down to 58% and
143 277% to 26% respectively. Data for the maximum dry unit weight and optimum moisture content were
144 obtained using the developed compaction mould by Ali and Mohamed (2017). The data showed that

as the liquid limit of the clay material was lowered, an increased maximum dry unit weight and decreased optimum water content were recorded as illustrated in Table 2. Non-hydraulic high calcium hydrated lime that satisfied the requirements of BS EN 459-1 was used. About 97 to 99.5% of lime powder is finer than 90 microns. The availability of lime in the form of calcium hydroxide ranges from 95 to 97%.

Table 1: Chemical analysis of primary clays

Component, %	Bentonite clay	Ball clay
SiO_2	63.02	52.0
Al_2O_3	21.08	31.5
Fe_2O_3	3.25	1.0
K_2O	-	2.3
Na_2O	2.57	0.3
MgO	2.67	0.4
CaO	0.65	0.2
FeO	0.35	-
TiO_2	-	1.1
L.O.I. @ 1000C*	5.64	11.3
Carbon	-	1.6
Trace	0.72	-

Table 2: Geotechnical properties for utilised clay materials

		Material			
		M1	M2	M3	M4
Composition*	Bentonite clay (%)	100	0	25	50
	Ball clay (%)	0	100	75	50
Liquid limit (%)		320	58	115	189
Plastic limit (%)		43	32	36	40
Plasticity Index (%)		277	26	79	149

Maximum dry unit weight (kN/m^3)	12.16	14.14	13.48	12.95
Optimum moisture content (%)	40	29	32.5	37.5

*The ratio of Bentonite to Ball clay is by mass.

2.2 Test procedure and programme

In order to minimise potential scattering of UCS results, full attention was given to the experimental procedure in order to avoid possible sources of the scattering including; i. adopting a cautious and thorough mixing technique to eliminate the formation of lime lumps, to ensure a high degree of pulverisation and to reduce the disparity in mixing time, ii. selection of a feasible and efficient compaction method to ensure the uniformity of dry density throughout the specimens and repeatability of specimens and iii. conduction of a curing protocol that provided a stable and constant curing temperature and humidity to avoid partial drying out of specimens. It should be noted that an identical procedure was followed for the preparation of all specimens. Each mixture was prepared by adding a predetermined amount of clay with the intended amount of lime and mixed mechanically. Then, a given amount of water was added, and the mixing was continued manually to distribute the water as uniformly as possible at this stage. Subsequently, the mixture was passed through the 2 mm sieve. Immediately, the retained clay-lime mix was kneaded by hand and passed through the same sieve. The mixture was then re-mixed mechanically to ensure homogeneity. In order to avoid the adverse impacts of the mellowing period, all mixtures were compacted directly after finishing the mixing process. All mixtures were compacted statically in five layers to produce specimens with a diameter of 38 mm and a height of 76 mm. Specimens were prepared to achieve a designated maximum dry unit weight at the optimum moisture content as illustrated in Table 2 using the developed compaction mould and the compaction procedure by Ali and Mohamed (2017). The adopted compaction method was found to be effective and efficient in preparing specimen with less than 4% scattering in UCS results (Ali and Mohamed, 2017). This shows a remarkable degree of improvement in reducing the UCS results than the 10% recommended acceptable scattering by (Consoli et al., 2011). Upon completion of compaction, specimens were extracted from the mould and

177 measurements of specimen's mass, and dimensions were taken. Each Specimen was then wrapped
178 properly using a cling film and placed in a double sealed bag. The specimens were then stored in an
179 environmental cupboard at the desired temperature of 20°C or 40°C and 90% relative humidity for
180 curing except those that were tested immediately after the compaction process. Table 3 presents the
181 full details of the experimental programme. In total, 336 specimens were prepared to assess the effect
182 of different parameters. Also, 140 specimens were prepared as replicates for quality assurance of UCS
183 values and to confirm the effectiveness of preparation method in alleviating the scattering in the
184 results especially with curing time of 168 h and 672 h. Results of UCS on replicate specimens showed
185 that the scattering in the results did not exceed the 4% even with prolonged curing time. All UCS tests
186 were performed using an automatic loading machine. Data for the axial strain and axial stress were
187 registered automatically every second. The loading velocity at which specimens were tested was
188 1mm/min.

189 Table 3: Testing programme

Series	Material	Parameters		
		Variables	Fixed	Note
1	M1	C = 0, 3, 6, 12, 24, 48, 72, 168 and 672 h T = 20°C and 40°C L = 5, 7, 9, 11 and 13%	γ_d = 12.16 kN/m^3 MC= 40% MP = 0 h	Additional specimens for L = 11% after 192 & 216 h and L = 13% after 96, 216, & 240 h at 40°C
2	M1	C = 0, 3, 6, 12, 24, 48, 72, 96, 144, 168, & 672 h T = 20°C and 40°C L =17, 23 and 25%	γ_d = 12.16 kN/m^3 MC= 40% MP = 0 h	Excessive lime content Additional specimens for L = 17% after 216 h, L =21% after 192 & 240 h and L = 25% after 240 & 288 h at 40°C
3	M2	C = 0, 24, 48, 72, 168 and 672 h T = 20°C and 40°C L = 5, 7, 9, 11 and 13%	γ_d =14.14 kN/m^3 MC= 29% MP = 0 h	Additional specimens for all lime contents after 3 h at 40°C

4	M3	C = 0, 24, 48, 72, 168 and 672 h T = 20°C and 40°C L = 5, 7, 9, 11 and 13%	γ_d =13.48 kN/m^3 MC = 32.5% MP = 0 h	Additional specimens for all lime contents after 3 h at 40°C
5	M4	C = 0, 24, 48, 72, 168 and 672 h T = 20°C and 40°C L = 5, 7, 9, 11 and 13%	γ_d =12.95 kN/m^3 MC = 37.5% MP = 0 h	Additional specimens for all lime content after 3 h at 40°C

where; C = curing time, MP = mellowing period, L = lime content, T = temperature, MC = moisture content and γ_d = Dry unit weight

3. Results and discussion

3.1 M1 Clay (Bentonite clay)

The strength values for all lime treated bentonite specimens that were tested immediately after compaction were higher than double the strength value of the untreated specimen, which was 0.5 MPa. The sudden increase in the strength of lime stabilised bentonite is consistent with earlier observations by Vitale et al. (2017). This increase could be caused by a reduction in the specific surface area which can be attributed to the flocculation and aggregation mechanisms that were prompted by cation exchange phenomena and enhanced by the immediate formation of initial cementitious compounds that takes place instantly after the addition of lime in the presence of water.

The evolutions of strength gain over the curing period at different temperatures of 20°C and 40°C are illustrated in Figure 1 and 2, respectively. The figures revealed that the evolution of strength passes through two phases, depending on the rate of strength gain and can be named first and second phases. During the first phase, the rate of strength gain was extremely high compared with that recorded in the second phase in particular at the higher temperature. The first phase can then be defined as the interval of time after which the rate of strength gain commences to slacken drastically.

Due to the role that the higher temperature of 40°C plays in accelerating the strength gain and thus the lime consumption, it is easier to distinguish the onset of the second phase at the higher temperature, unlike at the temperature of 20°C.

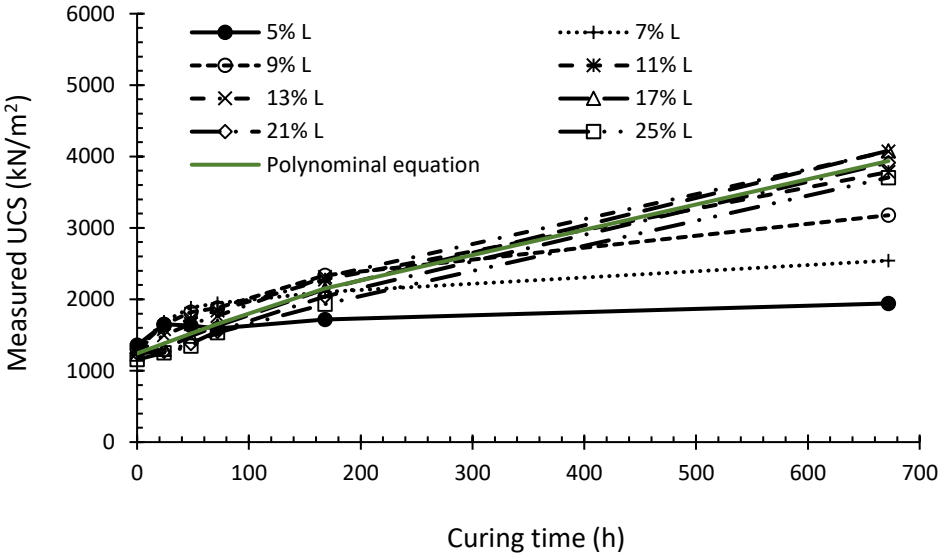

Figure 1: Evolution of strength gain with time for lime treated M1 specimens cured at 20°C

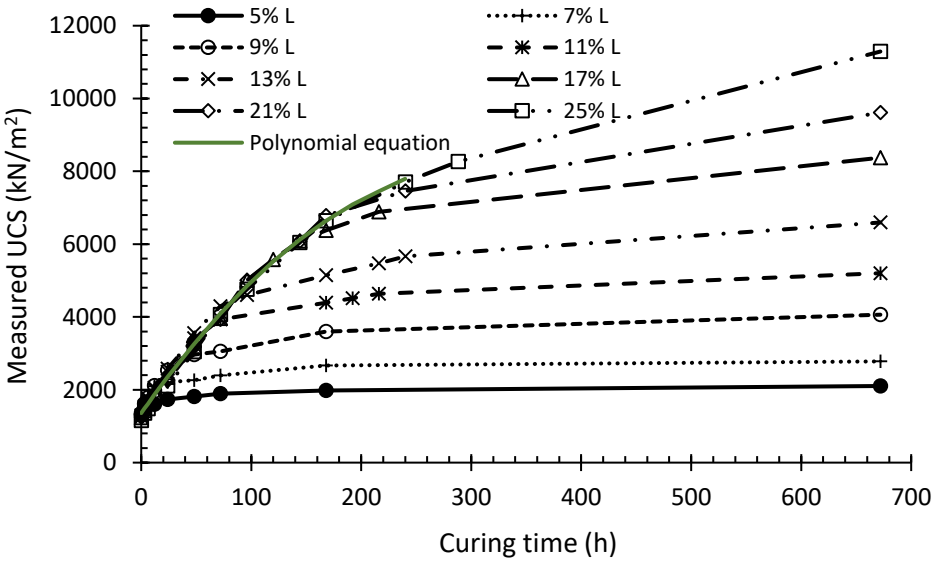

Figure 2: Evolution of strength gain with time for lime treated M1 specimens cured at 40°C

Although the strength gain appeared to develop remarkably over the first phase, the rate of strength gain slightly decreased as time elapsed. Therefore, a polynomial equation was found to best describe

217 the strength gain over the first phase. The best fit lines that are plotted in Figures 1 and 2 represent
218 the polynomial relationships that govern the strength evolution at 20 and 40°C, respectively. At 40°C,
219 the strength gain during the first phase can be given by the Equation 1 until 6, 24, 48, 72, 96, 144, 192,
220 and 240 h on specimens with lime content of 5, 7, 8, 9, 11, 13, 17, 21 and 25% respectively.

$$\mathrm{UCS}_{\mathrm{First\ phase}} = -0.0674\mathrm{C}^2 + 42.77\mathrm{C} + 1360.6 \quad \mathrm{R}^2 = 0.99 \qquad 1$$

221 The data suggested that the continuity of the first phase was strongly dependent on the lime content,
222 and its duration increased with the increase in the lime content. Here it should be mentioned that
223 higher lime contents from 17 to 25% were considered to assess the continuity of the first phase.

224 However, the data showed that the strength of lime stabilised bentonite during the second phase can
225 be represented by logarithmic relationship reaching strength values of 2, 2.78, 4, 6.6, 8.37, 9.6 and
226 11.3 MPa after 672 h of curing time for lime contents of 5, 7, 9, 11, 13, 17, 21 and 25% respectively.
227 Unlike the relatively shorter first phase at 40°C, the results showed that the first phase at 20°C
228 continued to 672 h with the addition of the substantial amount of lime, e.g. 11, 13, 17, 21, and 25%
229 reaching nearly a strength value of about 4 MPa. In contrast, the first phase was shorter with the
230 addition of 5, 7 and 9% of lime at 20°C achieving 2, 2.5 and 3.1 MPa respectively but it was reached
231 after extremely long periods of curing time in comparison with those recorded at 40°C on specimens
232 treated with the same lime content. During the first phase at 20°C, the strength is governed by
233 Equation 2.

$$\mathrm{UCS}_{\mathrm{First\ phase}} = -0.0028\mathrm{C}^2 + 5.89\mathrm{C} + 1242.6 \quad R^2 = 0.98 \qquad 2$$

234 However, careful inspection of data presented in Figure 2 on specimens cured at 40°C suggested that
235 most of the difference in the strength was gained during the first phase and was a function of the lime
236 content. The rate of strength gain during the second stage was significantly lower but increased with
237 the further addition of lime. In an attempt to describe the evolution of strength over phase 2 at 40°C,
238 Equation 3 was developed based on the attained data. The strength given by Equation 3 evolves
239 logarithmically as a function of lime content (L) and curing time (C) during phase 2 at 40°C.

$$UCS_{Second\ phase} = (4L^2 + 41.9L - 235)ln\ C + (-35.1L^2 + 464.1L - 87.1) \quad 3$$

To aid the discussion on examining the lime consumption, Figure 3 was plotted to present the attained strength results on specimens after 672 h of curing time against the lime content at 40°C and 20°C. The data attained on specimens cured at 40°C showed that there was a linear relationship between strength and lime content up to a lime content of 13% and that the difference in the strength value between two consecutive lime contents was about 1 MPa. This means that the amount of lime was fully consumed within the 672 h of curing time under 40°C. Extrapolating the best fit line at higher lime content would assist with the estimation of the final strength at the time of full consumption of lime. The best fit line for the full range of lime content used in this investigation was plotted in Figure 3. The resulting linear equation (Equation 4) from this relationship was used to predict the presumed final strength for other lime contents of 17, 21 and 25%.

$$\mathrm{UCS_{Presumed\ final\ strength}} = 546.2\mathrm{L} - 791 \quad 4$$

The values showed that at 40°C the available lime was wholly consumed during the 672 h of curing time on specimens with lime content up to 17% whereas specimens with lime content of 21% and 25% might not have fully consumed the lime. Furthermore, data attained on specimens that were cured at 20°C indicated that just lime contents of 5 and 7% were nearly consumed whereas other lime contents would require a prolonged period of curing time more than 672 h to consume the available lime. The data suggested that the addition of lime of more than 13% would remain unconsumed in the stabilised clay when cured at 20°C.

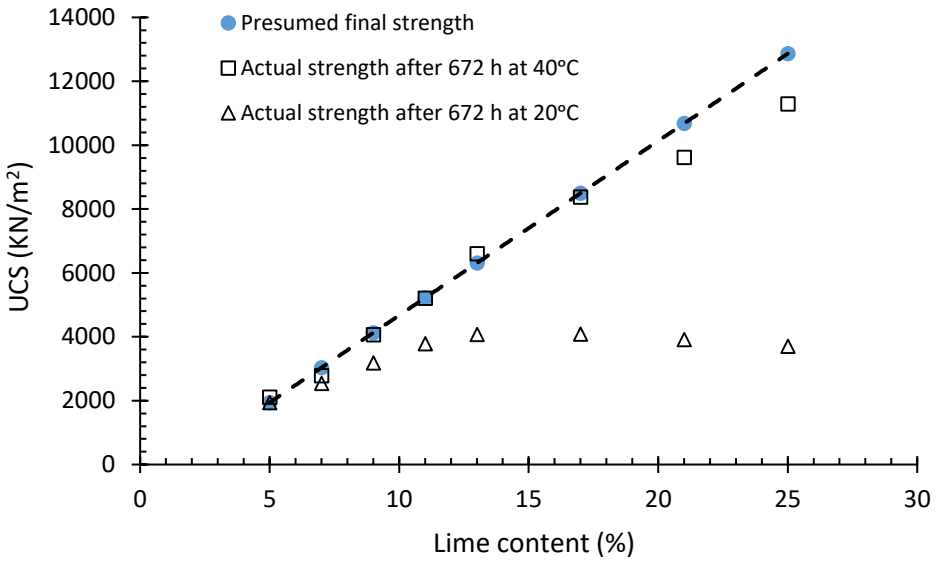

257

258 Figure 3: comparison between the presumed final strength and measured strength after curing for
259 672 h at 20°C and 40°C on specimens of treated M1 clay.

260

261 3.2 M2 Clay (Ball clay)

262 Results on the specimens that were tested directly after compaction process showed attainment of
263 UCS strength of 0.82, 0.89, 0.92, 0.95, and 1.03 MPa for 5, 7, 9, 11 and 13% of lime contents
264 respectively compared with just 0.33 MPa for untreated specimens. This illustrated that the addition
265 of lime could also enhance the strength of kaolinite material to up to 3 times in comparison with the
266 strength of untreated clay. The sudden surge in strength could be attributed to the fast initial calcium
267 adsorption and sodium desorption in cation exchange process within the first five minutes on kaolinite
268 soil which was reported by (Singh et al., 1996; Chemeda et al., 2018). Chemeda et al. (2018) also
269 observed that as the concentration of $Ca(OH)_2$ increased, the adsorbed calcium by Kaolinite became
270 higher according to measurements taken for the calcium concentration after 3 h from submerging
271 equal amounts of kaolinite in various concentration of $Ca(OH)_2$.

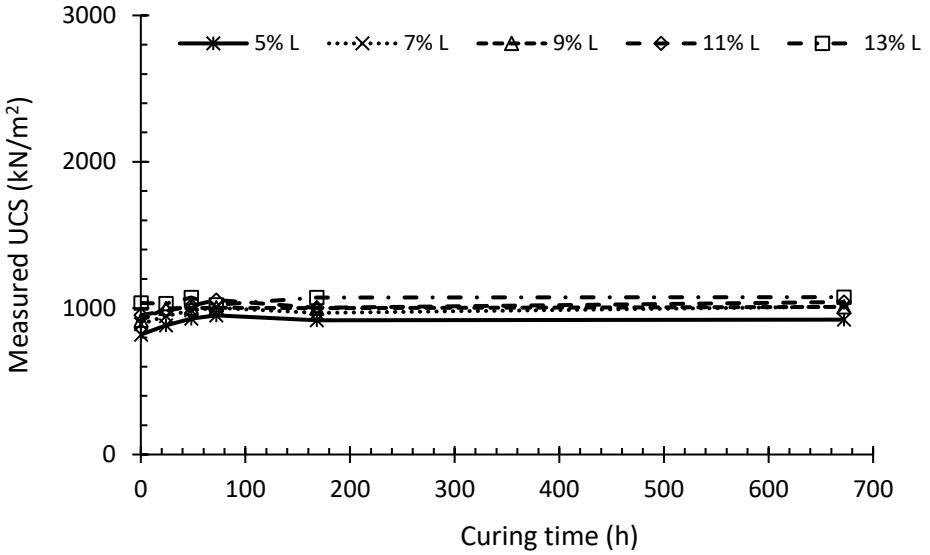

272

273 Figure 4: Evolution of strength gain with time for lime treated M2 specimens at 20°C

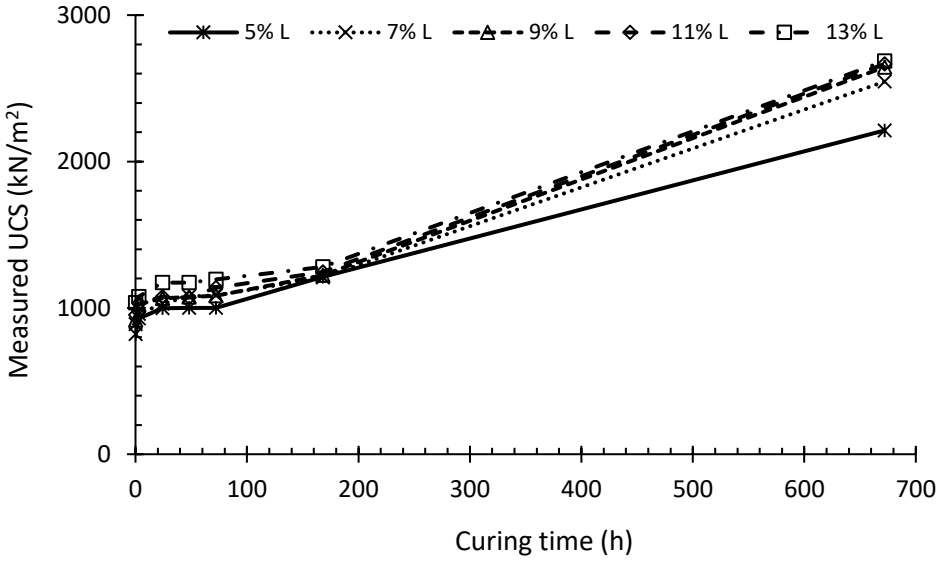

274

275 Figure 5: Evolution of strength gain with time for lime treated M2 specimens at 40°C

276 The evolution of strength gain for lime treated kaolinite specimens under a temperature of 20°C and
277 40°C were plotted against the curing time in Figures 4 and 5 respectively. The attained strength values
278 on specimens that were cured at 20°C indicated a very marginal increase in the strength within the
279 first 72 h subsequently the strength remained constant irrespective of the lime content and curing
280 time as seen in Figure 4. This would be due to a delay in the consumption of lime and the absence of
281 formation of cementitious compounds after treating kaolinite clay, which was observed by Vitale et

al. (2017). Though, Bauer and Berger (1998) reported that in alkaline solution, the dissolution rate of kaolinite was higher than its counterpart with the bentonite. (Konan et al., 2009; Chemeda et al., 2015; Chemeda et al., 2018) attributed the observed behaviour of kaolinite to the accumulation of various adsorbed calcium species on the surfaces of kaolinite mineral forming a coating layer which isolates the surface of the kaolinite clay particles from the alkaline environment, curbs the dissolution of alumina and silica compounds and thus inhibits the pozzolanic reaction. In contrast, when curing at 40^{o}C, the strength remained nearly stable during the first 72 hours followed by a gradual but remarkable gain in the strength up to reaching values of 2.2, 2.54, 2.6, 2.66 and 2.68 MPa for 5, 7, 9, 11 and 13% of lime content respectively after 672 h as illustrated in Figure 5. This gave a clear indication of the temperature role (40^{o}C) in accelerating the strength gain. Furthermore, the lowest strength value for 5% lime content indicated that the available lime content was nearly consumed during the 672 h (28 days) of curing at 40^{o}C. The role of higher temperature, e.g. 50^{o}C in re-initiating the strength gain in lime-treated kaolinite after a period of stability (7 days) was also reported by Maubec et al. (2017). Maubec et al. (2017) coupled this behaviour with the re-initiation of the calcium absorption and the beginning of forming hydrates compounds, e.g. Calcium Aluminate Hydrates and Carboaluminate Hydrates. However, the mechanism by which the accumulating calcium layer is eliminated, after a long time at 20^{o}C and shorter time at 40^{o}C, so that the alkaline environment could attack the surface of kaolinite, has not been clarified yet. A possible elucidation could be referred to the calcium disposal mechanisms which depend on the specific surface area of kaolinite over time at 20^{o}C that showed a prolonged increase as observed by Vitale et al. (2017). Whereas a relatively faster increase in the specific surface area at 40^{o}C is likely to occur, which enables the accommodation of the calcium accumulation. Further investigations would be needed to assess the evolution of specific surface area over time at different temperature.

307 3.3 M3 Clay (a mix of 1 portion of Bentonite to 3 portions of Ball clay)

308 The UCS data attained on M3 specimens treated with 5, 7, 9, 11 and 13% of lime and cured for a period
309 of time up to 672 h at 20°C and 40°C are shown in Figures 6 and 7, respectively. Immediately after
310 compaction, the UCS was nearly equal for all specimens irrespective of the lime content and was about
311 double of the UCS of the untreated specimen (0.5 MPa). Unlike lime treated Ball specimens, the
312 treated M3 specimens showed marginal strength gain of about 0.4 MPa after 672 h at 20°C, reaching
313 UCS value of about 1.4 MPa for all specimens. Equation 5 governs the evolution of strength during the
314 initial phase at 20°C.

$$\mathrm{UCS}_{\mathrm{First\ phase}} = -0.0003\mathrm{C}^2 + 0.78\mathrm{C} + 1031.5 \quad \mathrm{R}^2 = 0.96 \qquad 5$$

315 In contrast, the cured specimens at 40°C achieved UCS values of 1.4 MPa in only 48 h, which
316 highlighted the significant role for the curing temperature in accelerating the chemical reaction. After
317 a period of curing of 168 h at 40°C, the measured UCS values for all specimens with different lime
318 contents were nearly the same at about 2.1 MPa except a specimen that was treated with 5% lime
319 content which showed a slowdown in the strength gain entering in the second phase after 72 h of
320 curing. The UCS values observed on specimens with 5% lime content experienced no appreciable
321 change after 168 h of curing achieving a value of almost 1.9 MPa. The no significant change in the
322 strength suggests that the addition of 5% lime is not enough to support further reactions between
323 lime and clay after 168 h of curing at 40°C. The UCS values at 40°C increased notably with the increase
324 in lime content reaching 2.7, 3.6, 4.0 and 4.2 MPa on M3 specimens treated with lime content of 7, 9,
325 11 and 13% respectively after 672 h of curing. Equation 6 governs the evolution of strength during the
326 initial phase at 40°C.

$$\mathrm{UCS}_{\mathrm{First\ phase}} = -0.0039\mathrm{C}^2 + 7.13\mathrm{C} + 1072 \quad \mathrm{R}^2 = 0.99 \qquad 6$$

327 Results of measured UCS values at 672 h of curing time were plotted against lime content in Figure 8.
328 The data suggested that UCS values attained at 672 h at 40°C is directly related to the lime contents
329 of 5, 7, and 9%, which means that lime was fully consumed during the curing period. Consequently, a

linear relationship (Equation 7) between UCS and lime content is obtained and used to predict the final UCS values for specimens treated with higher lime contents of 11 and 13%.

$$\mathrm{UCS}_{\text{Presumed final strength}} = 405.7\mathrm{L} - 115.9 \qquad 7$$

Comparing estimated strength values with measured UCS values after a period of curing of 672 h at 40°C illustrated that specimens treated with 11 and 13% of lime would not have reached their maximum strength yet which means that lime might not be fully consumed. Nevertheless, curing at 20°C slowed the consumption of lime and resulted in markedly lower values of strength. In addition, the relationship indicated that a 1% increase in the lime content would result in an increase of 0.4 MPa in the final strength value when cured at 40°C.

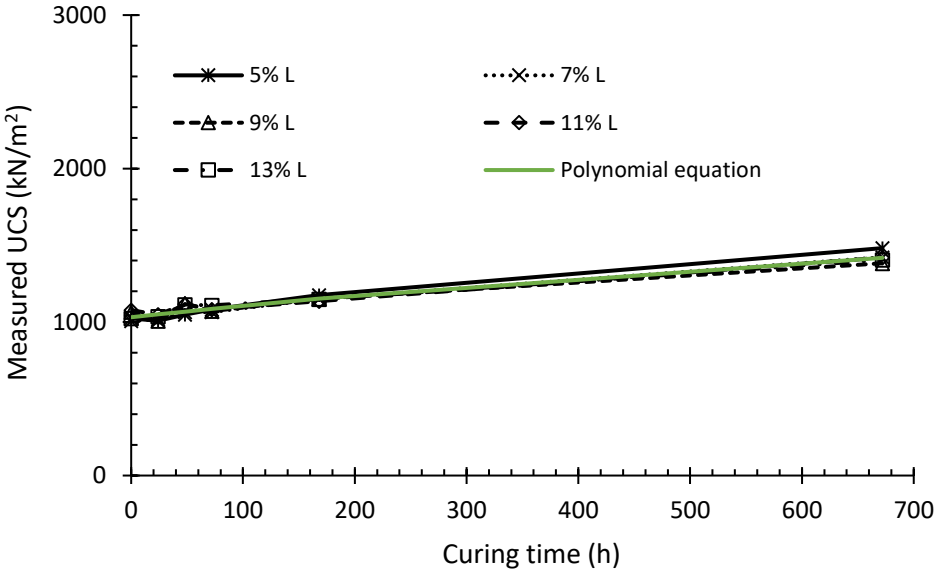

Figure 6: Evolution of strength gain with time for lime treated M3 specimens at 20°C

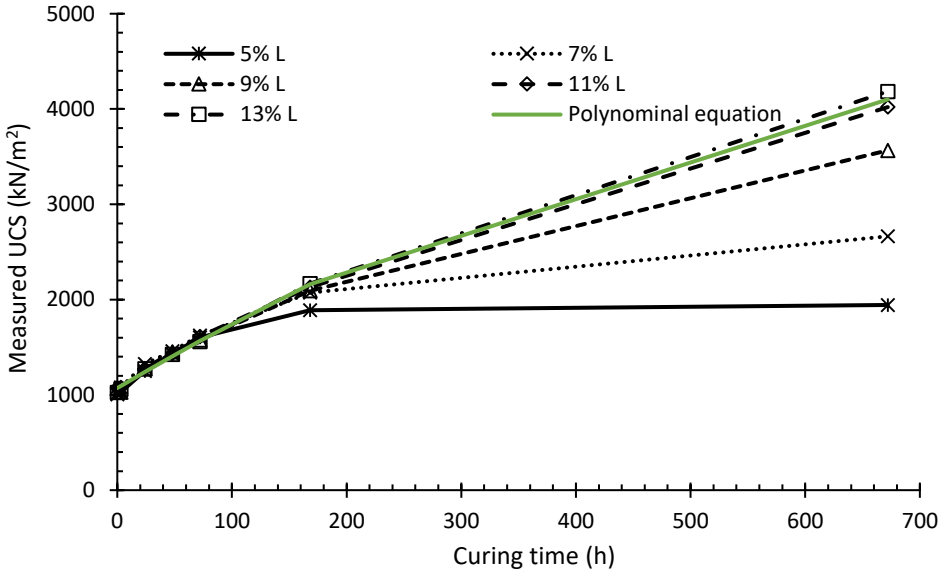

340

341 Figure 7: Evolution of strength gain with time for treated M3 specimens at 40°C

342

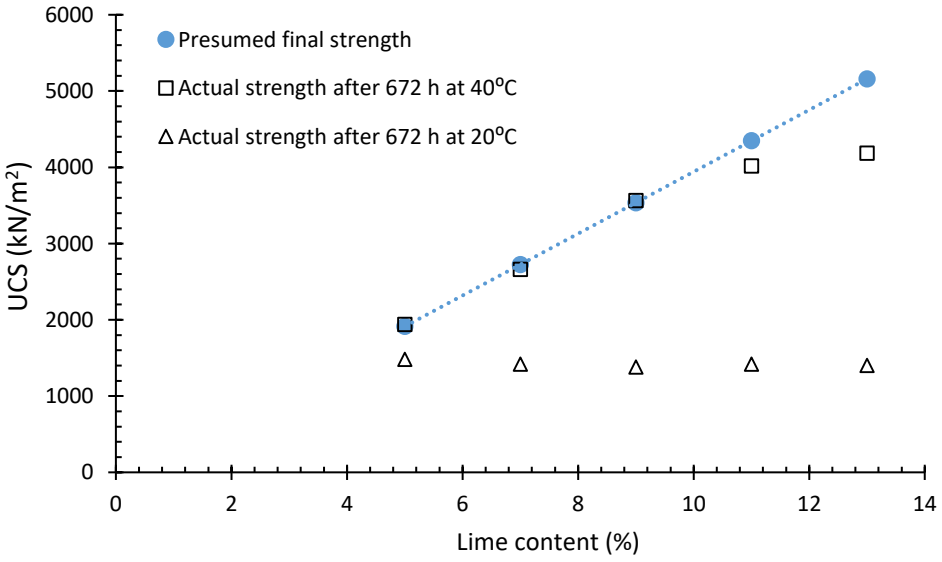

343

344 Figure 8: comparison between the presumed final strength and the measured strength after curing

345 for 672 h at 20°C and 40°C for treated M3 specimens

346

347

348

349 3.4 M4 Clay (A mix of 1 portion of Bentonite to 1 portion of Ball clay)

350 The UCS evolution of compacted M4 specimens that were treated with 5, 7, 9, 11 and 13% of lime and
351 cured for a period of time up to 672 h at 20°C and 40°C are depicted in Figures 9 and 10 respectively.
352 The measured UCS values for all treated specimens that tested directly after compaction were about
353 two times that attained on the untreated specimen (0.43 MPa). Results of UCS on specimens treated
354 with 7, 9, 11 and 13% of lime and cured at 20°C showed a gradual increase in strength over the whole
355 duration of curing. This means that the first strength phase continued until 672 h for specimens with
356 lime content of 7% and higher. The relationship between strength and curing time seems to be
357 governed by the polynomial Equation 8, achieving the same UCS value of about 2.2 MPa at 672 h.
358 However, M4 specimens treated with 5% lime did not follow the same path for the evolution of
359 strength. The strength did not increase after 168 h of curing time, indicating the commencement of
360 the second phase.

$$\mathrm{UCS}_{\text{First phase}} = -0.0015\mathrm{C}^2 + 2.8\mathrm{C} + 1059.9 \quad \mathrm{R}^2 = 0.99 \qquad 8$$

361 On the other hand, specimens cured at 40°C showed a typical relationship through which the strength
362 gain was initially fast followed by a slower second phase. It is clear that the continuity of the fast phase
363 was dependent on the availability of lime. The strength gain over the first phase at 40°C is governed
364 by Equation 9. The achieved strength at the end of curing period at 40°C was directly related to the
365 lime content attaining 2, 2.9, 4.2, 4.9 and 5.8 MPa on specimens treated with lime content of 5, 7, 9,
366 11 and 13% respectively.

$$\mathrm{UCS}_{\text{First phase}} = -0.043\mathrm{C}^2 + 22.52\mathrm{C} + 1089 \quad \mathrm{R}^2 = 0.99 \qquad 9$$

367

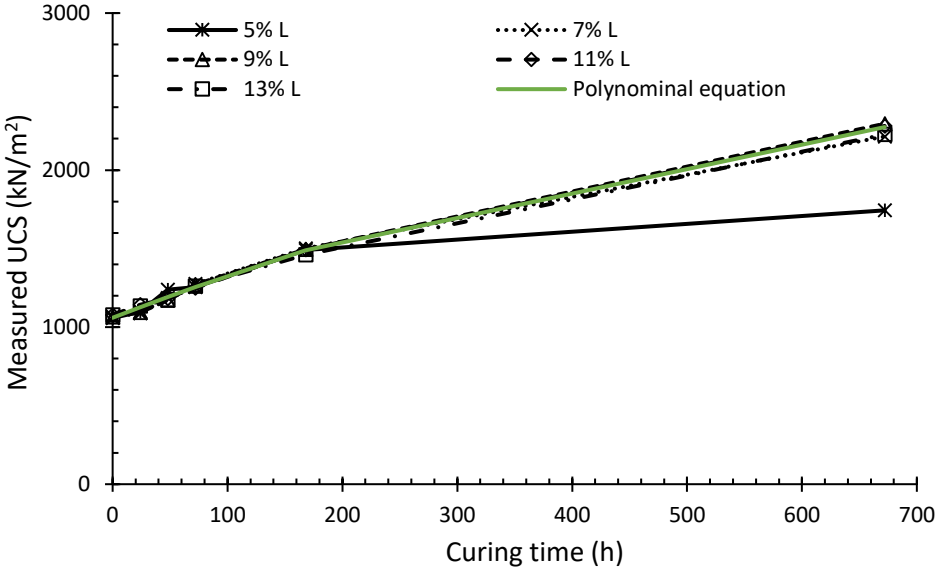

368

369 Figure 9: Evolution of strength gain with time for M4 specimens at 20°C

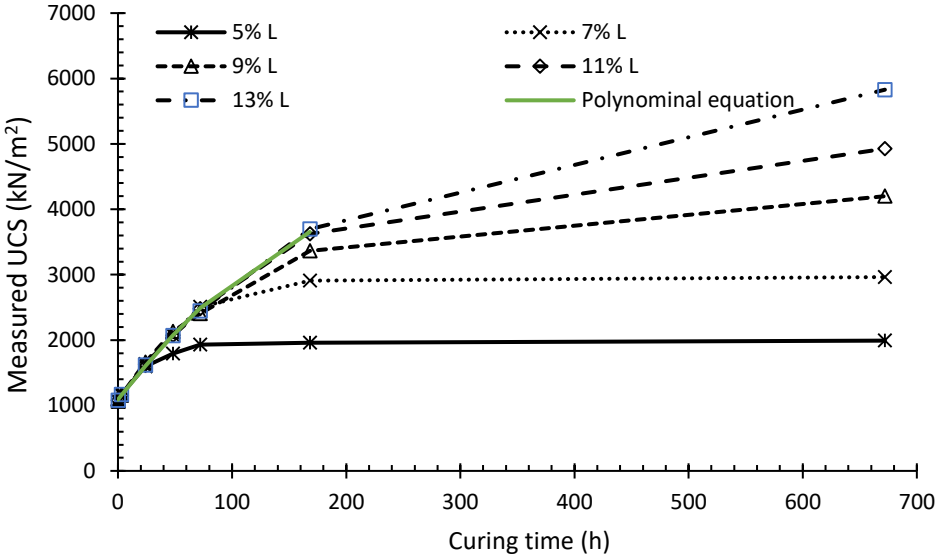

370

371 Figure 10: Evolution of strength gain against curing time for M4 specimens at 40°C

372 The attained UCS at 20 and 40°C after 672 h of curing were plotted in Figure 11 against the
373 corresponding lime content. The data suggest that lime would be consumed entirely on specimens
374 treated with lime content of 5, 7 and 9% at 40°C since Equation 10 can fit the data accurately.
375 Extending the linear equation (Equation 10) to higher lime contents indicated that the higher lime
376 content need further curing time to be completely consumed even at ambient temperature of 40°C.

The best fit line indicated that after 5% of lime content, an increase of 1% in the lime content would result in an increase in the final strength value by about 0.55 MPa. The data suggest that lime was not consumed when specimens were cured at 20°C. The data in Figures 3, 8 and 11 highlighted the responsibility of lime content on determining the final strength value and the role of mineralogy composition and temperature on determining the time needed to reach the final value. It was also noticed that each increase of 1% lime above 5% lime content offers an increase in the final strength ranging from 0.4 to 0.55 MPa.

$$\mathrm{UCS}_{\text{Presumed final strength}} = 552.15\mathrm{L} - 813.15 \qquad 10$$

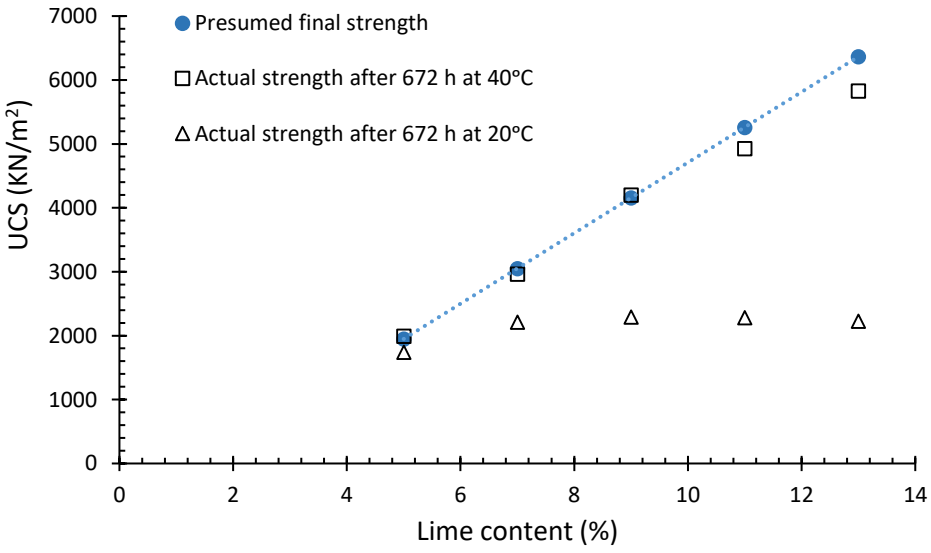

Figure 11: comparison between the presumed final strength and measured strength after curing for 672 h at 20°C and 40°C for treated M4 clay

3.5 Mineralogical effects

In this investigation, four different types of clay namely; M1 of pure bentonite, M2 of pure kaolinite, M3 which is a mix of Bentonite and Kaolinite with a ratio of 1:3 by mass and M4 which is a mix of Bentonite and Kaolinite with a ratio of 1:1 by mass were used to represent soils with a vast range of

393 liquid limit from 330% down to 58%. Based on the UCS results that were presented earlier for the four
394 different types of clay, thorough assessment and comparison were conducted to highlight the impact
395 of clay mineralogy on the reaction process and kinetics of strength gain when mixed with hydrated
396 lime.

397 The data showed that testing lime treated specimens with a range of lime contents immediately after
398 compaction would result in a relatively narrow range of UCS values. By and large, the UCS values on
399 treated specimens were 2~3 times that achieved on untreated specimens irrespective of the amount
400 of added lime. The UCS values increased slightly with the increase in the bentonite content in the
401 specimens. The immediate changes in the structure and bonding between treated particles could be
402 attributed primarily to cation exchange, flocculation and aggregation mechanisms and enhanced by
403 the immediate formation of initial cementitious compounds. Since the surface area of bentonite clay
404 is much higher than that of kaolinite clay, it is more likely that the lime would react with the bentonite
405 particles at a higher rate resulting in a significant reduction in the surface area of bentonite and in a
406 relatively higher strength immediately after compaction. The results demonstrated that the amount
407 of added lime at zero h curing has no impact on the evolvement of strength which could be attributed
408 to the small amount of lime that is required to satisfy the needs for cation exchange and flocculation
409 mechanisms.

410 Careful inspection of UCS data for all clays indicated that the kinetic of strength gain throughout curing
411 is dependent on curing temperature, lime content and curing time. Two stages were very noticeable
412 in the evolution of strength of the lime-treated clays in particular at the high temperature of 40^{o}C.
413 Quadratic equations were proposed for stage 1 of strength gain (fast-growing) and presented in
414 Figures 2 and 3 for the bentonite clay. It was noted that during the first days of curing both equations
415 behave mostly linear due to the small negative value of the numerical coefficient in the second order
416 parameter compared with the higher positive numerical coefficient in the first order parameter. So, it
417 can be inferred that the numerical coefficients in the first order parameters reflect the kinetic of

418 strength gain under both temperatures. Consequently, the results suggested that during the first
419 hours (stage 1), the kinetic of strength gain at curing temperature of 40°C was about 8 times that
420 experienced when curing at 20°C.

421 To appreciate the effect of bentonite inclusion with the Ball clay, the kinetic of strength gain of lime-
422 treated treated M3 and M4 were also assessed using the numerical coefficients in the quadratic
423 equations (5, 6, 8 and 9) (. Discarding the minor numerical coefficients in the second order parameters,
424 it became clear that the strength gain was a function of the clay mineralogy and increased with
425 elevating the curing temperature as seen in Figure 12. The kinetic of strength gain of M3 and M4
426 experienced at curing temperature of 40°C was found to be also about 8 times that recorded when
427 curing at 20°C. At a given temperature, the rate of strength gain with M3 and M4 during stage 1 was
428 about 15% and 50% of that recorded for M1 which highlighted a significant role of the bentonite in
429 the reaction with lime and evolution of strength.

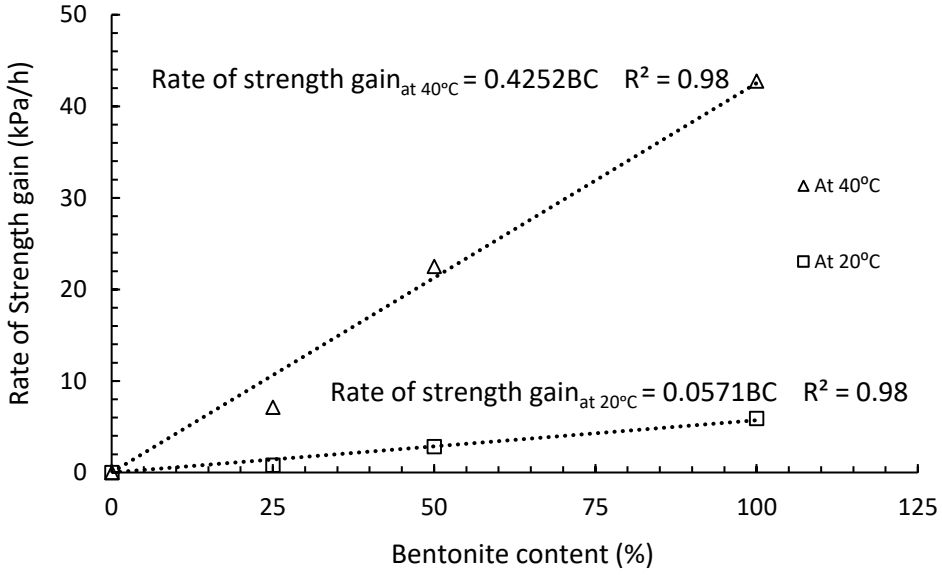

430

431 Figure 12: impact of Bentonite Content (BC) on the kinetic of strength gain during the first phase at
432 different curing temperatures

433 Two possible elucidations could be brought forward to clarify the changes leading to the increase in
434 strength gain with the increase in the bentonite content; i. increasing the amount of bentonite content

435 pushes towards consideration that bentonite is predominantly responsible for the degree of
436 improvement in the strength gain since the increase in strength is directly related to the proportional
437 of bentonite in the material and ii. bentonite might act as a rival consumer for calcium ions in the lime
438 leading to reduced accumulation of calcium ions on the surface of kaolinite particles. Consequently,
439 the alkaline environment was allowed access to the surface of kaolinite layer. As a result of attacking
440 the alkaline environment to the surface of kaolinite and montmorillonite minerals, silica and alumina
441 would be released leading to the formation of cementitious compounds in the form of Calcium Silicate
442 Hydrates (CSH), Calcium Aluminate Hydrates (CAH) and Calcium Aluminate Silicate Hydrates (CASH).
443 It is well known that kaolinite minerals comprise of the octahedral sheet (AL site) and tetrahedral
444 sheet (Si site) whereas, in the case of montmorillonite, there are two tetrahedral sheets sandwiched
445 an octahedral sheet (Brigatti et al., 2006). Taking into account the differences in the structure of
446 minerals, the launch of alumina and silica would be synchronised in the case of kaolinite, and the
447 release of silica would be followed by the release of alumina in the case of montmorillonite minerals.
448 Bauer and Berger (1998) concluded that unlike the preference of releasing the silica in the case of
449 montmorillonite mineral, the preference of the dissolution of alumina was prevalent in the case of
450 kaolinite minerals. Using X-ray diffraction analysis, the presence of CAH with lime-treated kaolinite
451 was observed by Maubec et al. (2017) and Vitale et al. (2017) after 28 days at 20^{o}C, whereas CSH was
452 observed by (Maubec et al., 2017) after 98 days of curing at 50^{o}C. With respect to the montmorillonite
453 mineral, the presence of CSH was observed since the very short time of the treatment whereas the
454 presence of CAH and CASH were observed after a prolonged period of time as reported by (Pomakhina
455 et al., 2012; Vitale et al., 2016; Maubec et al., 2017; Vitale et al., 2017). Bauer and Berger (1998) also
456 reported that the rate of dissolution of kaolinite was higher than that in montmorillonite minerals in
457 a strong base solution (potassium hydroxide).

458 On the other hand, the results of two studies conducted by (Al-Mukhtar et al., 2010a; Al-Mukhtar et
459 al., 2010b) on expansive soils naturally contain 38% of kaolinite, and 58% of smectite minerals
460 indicated that the formation of CAH was observed using X-ray diffraction after 1 and 7 days at 50 and

20°C respectively. In contrast, the formation of CSH was observed at 50°C after 7 days. Hence, the availability of alumina and/or silica at the time when the reaction takes place controls the outputs of the pozzolanic reactions and the development of CAH, CSH and/or CSAH depending on the abundant reactants, e.g. alumina or silica (Beetham et al., 2015). The formation of CAH; 1. refers to the responsibility of kaolinite in the formation of the cementitious compounds and thus on the strength gain, 2. confirms the role that played by the smectite mineral as competitive consumer which prevents the accumulation of calcium ions on the surface of kaolinite and the faster dissolution of kaolinite in the alkaline environment. Based on that in the current study, it can be stated that the increase in bentonite content in M3 and M4 offered faster elimination of the calcium accumulation, the earlier appearance of cementitious compounds and initiation of greater kinetic of strength gain.

3.6 Collapse pattern and desiccation cracks

Careful inspection of the failure pattern of all lime-stabilised clay specimens suggested that the failure mechanism was markedly dependent upon the type of clay material and its strength which was a function of the amount of lime and curing conditions. Figure 13 shows pictures of specimens at failure after being cured for 672 h (28 days). In all specimens, the failure pattern was in the form of a cone-split that was well formed at one end only. The physical observations suggested that the cone-split equally occurred at either the top or the bottom of the specimens. Curing lime stabilised clays for a long period resulted in a brittle behaviour which can be noticed by failure at a relatively small strain of less than 2% as shown in Figure 14. The cone-split is very similar to that classified by ASTM C39 (2018), type 2 for the typical collapse in the cylindrical brittle concrete specimen.

a. M1
Lime treated bentonite
LP = 17% and T = 40°C

b. M2
Lime treated ball clay
LP = 13% and
T = 20°C

c. M3
Lime treated 1:3 bentonite – ball clay
LP = 9% and T = 40°C

d. M4
Lime treated 1:1 bentonite – ball clay
LP = 13% and T= 40°C

Figure 13: typical cone-split failure pattern on lime treated clays after 28 days

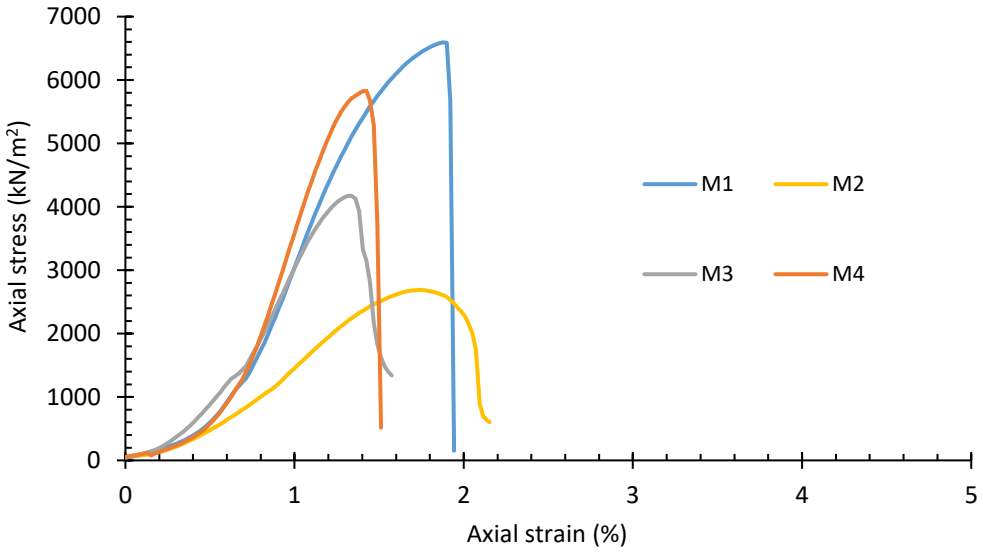

Figure 14: stress-strain relationships on lime treated clays: LP = 13%, T = 40°C and C = 672 h

Figure 15 shows an example of the failure of the M1 at different times of curing. It was observed that a classical shear collapse was imminent on specimens that were cured for a short period of time up to 12 h whereas a combined cone-shear collapse appeared to occur on specimens that were cured for a period of time between 12 and 72 h. Furthermore, the failure pattern on specimens cured for longer

periods showed a cone-split failure, as illustrated in Figure 15. The collapse pattern is related to the strength of the specimen at the time of testing, which is related to the type of clay and treatment and curing conditions. Results for the stress-strain relationships on treated M1 specimens at different curing times are presented in Figure 16. The results confirmed that the behaviour of lime treated clay specimens changed from ductile to brittle with the curing time. The ductile behaviour of lime-stabilised bentonite was accompanied by a classical shear failure, whereas the cone-split is dominant on high strength specimens that showed brittle behaviour.

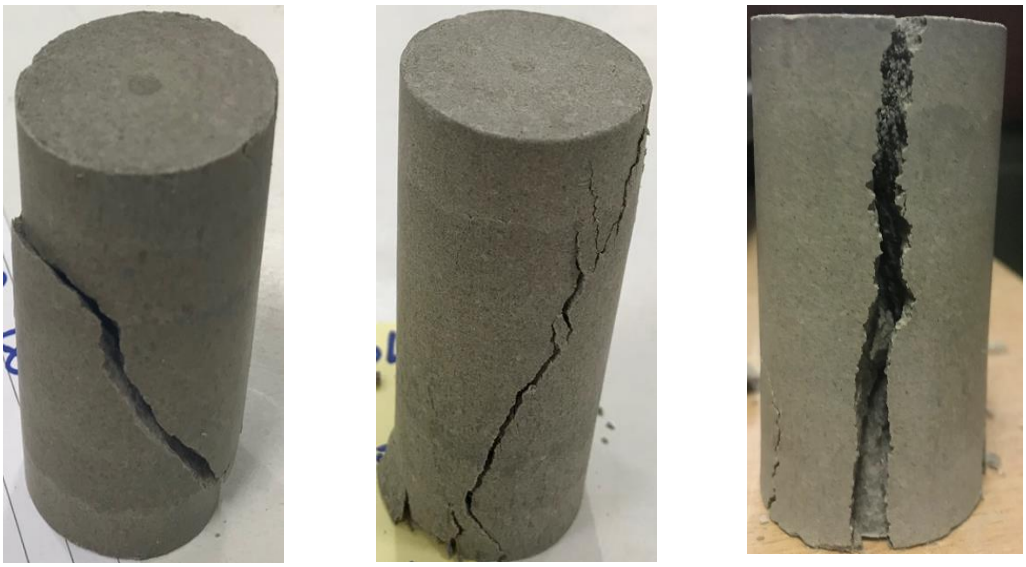

a. Shear collapse At zero curing time LP=21%

b. Cone-shear collapse At 24 h of curing at 40°C, LP=25%

c. Cone-split collapse after 72 h of curing at 40°C, LP=21%

Figure 15: the type of collapse patterns over the curing time on M1 specimens

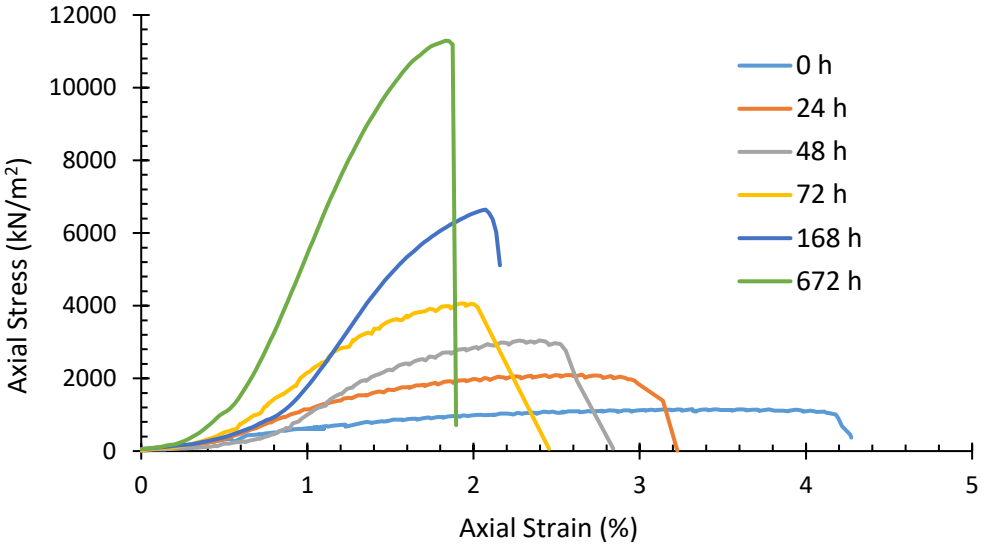

497

498 Figure 16: stress-strain relationships on lime treated M1 specimens as a function of curing time

499 Another distinctive feature was observed during the drying process during which all tested specimens
500 were dried in the oven at 105°C, to ascertain the water content of cured specimens. This was a final
501 quality assurance step that was important to ensure the effectiveness of controlling and maintaining
502 a target water content throughout the curing period. During the drying process, it was observed that
503 the appearance of desiccation cracks on the surface of lime treated bentonite (M1) is different from
504 that observed on lime treated ball clay (M2). The desiccation cracks on the lime-treated ball clay, M3
505 clay, and M4 clay specimens appeared at the onset of the drying process within 1 h (see figure 17a)
506 and then gradually closed by the end of 24 h of drying as shown in Figure 17b. Only some hair cracks
507 can still be visible on the specimens. Whereas the substantial amount of cracks were generated within
508 1 h of drying on lime treated bentonite M1 specimens (see, Figure 17 a) and some cracks were
509 widened with time and remained after completion of drying as shown in Figure 17b. Nevertheless,
510 there was no significant volume change on the lime-treated clays.

511

a. Treated M1 after 1 h of drying
b. Treated M1 after 24 h of drying
c. Treated M4 clay after 1 h of drying
d. Treated M4 clay after 24 h of drying

Figure 14: behaviour of desiccation cracks during the drying process of 7% lime treated clays: a and b for M1 clay and c and d for M4 clay

4. Conclusions

In this investigation, four different types of clay with a wide range of liquid limit were mixed with different amounts of lime up to 25% by mass to examine and evaluate the mineralogical effects on the chemical process and the evolution of strength. Five series of experiments were undertaken to test specimens with different lime contents at two different curing temperature for a period of curing time up to 28 days. The key outcome of the current investigation is that the beginning and vitality of changes in strength characteristic are related to the formation of cementitious compounds and its kinetics which depend primarily upon the mineralogy composition of clay and ambient temperature. Furthermore, at a given ambient temperature, the continuity of such changes in the characteristics of a given lime-treated clay depends on the availability of lime. In addition, several conclusions could be drawn out of the experimental study;

1. An immediate effect of lime on the strength of lime treated clays was evident in all specimens that were tested directly after compaction in comparison with those recorded on untreated

specimens at the same dry unit weight. The results suggested that an increase of 2 ~ 3 times could be achieved with the addition of lime. However, the degree of improvement in the strength was not related to the amount of lime.

2. Lime treatment of bentonite and kaolinite clays showed recognisable differences during the period of curing and immediately after the initial strength gain at zero h of curing period. Bentonite clay reacted swiftly with lime leading to a significant and sustained degree of improvement in the strength as time passed at 20^{o}C and 40^{o}C but with different rates. Nevertheless, specimens of treated Ball clay (Kaolinite) showed that the strength gain entered in an idle phase in which no growth in strength was observed over the 672 h of curing in particular at 20^{o}C. Whereas the idle phase was shortened to only 72 h when the curing temperature was raised to 40^{o}C.
3. Since the Ball clay comprised mainly of kaolinite minerals, the phenomenon of the accumulation of calcium cations species on the kaolinite surface caused obscuring the surfaces of mineral from the alkaline environment. This accumulation of calcium cations led to a delay in the release of alumina and silica and thus delaying the formation of cementitious compounds. However, the mechanism by which the accumulation of calcium was reduced or eliminated at 40^{o}C so that the alkaline environment was allowed to attack the surface of mineral and thus to launch the alumina and silica in order to form the cementitious compounds that are responsible for the strength gain, deserves further investigations.
4. The addition of Bentonite to Ball clay with a ratio of 1:3 and 1:1 to form M3 and M4 materials was found successful in eliminating the idle phase in the strength gain over the curing period. Bentonite would act as a competing consumer for the incoming calcium ions to the system reducing and/or eliminating the accumulation of the calcium ions on the surface of kaolinite minerals. This led to a gradual improvement in the strength but at a slower rate.
5. The results showed that the strength gain throughout curing went through two stages process. The first stage was recognised by a fast strength gain, followed by a second stage in

554 which a slower strength gain occurred. The two stages were very prominent at the high curing
555 temperature of 40°C. The time for stage 1 of strength gain was dependent upon the curing
556 temperature, lime content and mineralogy of clay. It increased with higher lime content and
557 increased bentonite portion.

558 6. Despite the use of quadratic equations to best fit stage 1 of strength gain, the numerical
559 coefficients for the second order term were found to be negligible. Simplifying the equations
560 into straight lines assisted with comparing the rate of strength gain.

561 7. During stage 1 of strength gain, the rate of strength gain at the high curing temperature of
562 40°C was found to be about 8 times that observed at the low curing temperature of 20°C. At
563 the same temperatures, the ratio between the rates of strength gain was very dependent
564 upon the clay mineralogy. The kinetic of strength gain of lime treated bentonite clay was about
565 2 and 7 times the kinetic of strength gain of lime treated clays with 50 and 25% bentonite
566 content, respectively.

567 8. The failure pattern was found to change throughout the curing period owing to the strength
568 of treated specimens. Classical shear failure was imminent on all specimens that were cured
569 for a short period up to 24 h. A combined shear and cone-split occurred on specimens that
570 were cured for up to 72 h and then cone-split failure pattern was observed on all specimens
571 that were cured for long periods. This was in harmony with the change in behaviour from
572 ductile to brittle with further curing.

573 **5. Acknowledgements**

574 This research did not receive any specific grant from funding agencies in the public, commercial, or
575 not-for-profit sectors.

576 **References**

577 Al-Alwan, A.A.K., 2019. Undrained shear strength of ultra-soft soils admixed with lime, University of
578 Glasgow.
579 Al-Mukhtar, M., Lasledj, A., Alcover, J.-F., 2010a. Behaviour and mineralogy changes in lime-treated
580 expansive soil at 20 °C. Applied Clay Science, 50(2): 191-198.
581 Al-Mukhtar, M., Lasledj, A., Alcover, J.-F., 2010b. Behaviour and mineralogy changes in lime-treated
582 expansive soil at 50 °C. Applied Clay Science, 50(2): 199-203.
583 Ali, H., Mohamed, M., 2017. The effects of compaction delay and environmental temperature on the
584 mechanical and hydraulic properties of lime-stabilized extremely high plastic clays. Applied
585 Clay Science, 150: 333-341.
586 Ali, H., Mohamed, M., 2018. The effects of lime content and environmental temperature on the
587 mechanical and hydraulic properties of extremely high plastic clays. Applied Clay Science,
588 161: 203-210.
589 Alrubaye, A.J., Hasan, M., Fattah, M.Y., 2018. Effects of using silica fume and lime in the treatment of
590 kaolin soft clay. Geomechanics and Engineering, 14(3): 247-255.
591 Aqoub, K., Mohamed, M., Sheehan, T., 2018. Analysis of sequential active and passive arching in
592 granular soils. International Journal of Geotechnical Engineering: 1-10.
593 ASTM C39, 2018. Standard Test Method for Compressive Strength of Cylindrical Concrete Specimens.
594 Bauer, A., Berger, G., 1998. Kaolinite and smectite dissolution rate in high molar KOH solutions at 35°
595 and 80°C. Applied Geochemistry, 13(7): 905-916.
596 Beetham, P. et al., 2015. Lime stabilisation for earthworks: a UK perspective. Proceedings of the
597 Institution of Civil Engineers - Ground Improvement, 168(2): 81-95.
598 Bell, F.G., 1996. Lime stabilization of clay minerals and soils. Engineering Geology, 42(4): 223-237.
599 Boardman, D.I., Glendinning, S., Rogers, C.D.F., 2001. Development of stabilisation and solidification
600 in lime–clay mixes. Géotechnique, 51(6): 533-543.
601 Bozbey, I., Garaisayev, S., 2010. Effects of soil pulverization quality on lime stabilization of an
602 expansive clay. Environmental Earth Sciences, 60(6): 1137-1151.
603 Brigatti, M.F., Galan, E., Theng, B.K.G., 2006. Structures and mineralogy of clay minerals,
604 Developments in clay science. Elsevier, pp. 19-86.
605 Chemeda, Y.C., Deneele, D., Christidis, G.E., Ouvrard, G., 2015. Influence of hydrated lime on the
606 surface properties and interaction of kaolinite particles. Applied Clay Science, 107: 1-13.
607 Chemeda, Y.C., Deneele, D., Ouvrard, G., 2018. Short-term lime solution-kaolinite interfacial
608 chemistry and its effect on long-term pozzolanic activity. Applied Clay Science, 161: 419-426.
609 Consoli, N.C., Lopes Jr, L.d.S., Prietto, P.D.M., Festugato, L., Cruz, R.C., 2011. Variables Controlling
610 Stiffness and Strength of Lime-stabilized Soils. Journal of Geotechnical and
611 Geoenvironmental Engineering, 137(6): 628-632.
612 Coudert, E., Paris, M., Deneele, D., Russo, G., Tarantino, A., 2019. Use of alkali activated high-calcium
613 fly ash binder for kaolin clay soil stabilisation: Physicochemical evolution. Construction and
614 Building Materials, 201: 539-552.
615 De Windt, L., Deneele, D., Maubec, N., 2014. Kinetics of lime/bentonite pozzolanic reactions at 20
616 and 50 C: Batch tests and modeling. Cement and Concrete Research, 59: 34-42.
617 Di Sante, M., Fratalocchi, E., Mazzieri, F., Pasqualini, E., 2014. Time of reactions in a lime treated
618 clayey soil and influence of curing conditions on its microstructure and behaviour. Applied
619 Clay Science, 99(0): 100-109.
620 Di Sante, M., Fratalocchi, E., Mazzieri, F., Pasqualini, E., 2019. Prediction of shear strength
621 parameters in soil–lime mixture design–part 1: quicklime. Proceedings of the Institution of
622 Civil Engineers-Ground Improvement: 1-12.
623 Diamond, S., Kinter, E.B., 1965. Mechanisms of soil-lime stabilization. Highway Research Record(92).
624 Gao, Y., Qian, H., Li, X., Chen, J., Jia, H., 2018. Effects of lime treatment on the hydraulic conductivity
625 and microstructure of loess. Environmental earth sciences, 77(14): 529.

626 Hashemi, M.A., Massart, T.J., François, B., 2018. Experimental characterisation of clay-sand mixtures
627 treated with lime. European Journal of Environmental and Civil Engineering, 22(8): 962-977.
628 Jahandari, S. et al., 2019. Experimental study of the effects of curing time on geotechnical properties
629 of stabilized clay with lime and geogrid. International Journal of Geotechnical Engineering,
630 13(2): 172-183.
631 Kang, G., Cikmit, A.A., Tsuchida, T., Honda, H., Kim, Y.-s., 2019. Strength development and
632 microstructural characteristics of soft dredged clay stabilized with basic oxygen furnace steel
633 slag. Construction and Building Materials, 203: 501-513.
634 Kitazume, M., Terashi, M., 2013. The deep mixing method. CRC press.
635 Konan, K.L. et al., 2009. Comparison of surface properties between kaolin and metakaolin in
636 concentrated lime solutions. Journal of Colloid and Interface Science, 339(1): 103-109.
637 Locat, J., Bérubé, M.-A., Choquette, M., 1990. Laboratory investigations on the lime stabilization of
638 sensitive clays: shear strength development. Canadian Geotechnical Journal, 27(3): 294-304.
639 Maubec, N., Deneele, D., Ouvrard, G., 2017. Influence of the clay type on the strength evolution of
640 lime treated material. Applied Clay Science, 137: 107-114.
641 Mirzababaei, M., Mohamed, M., Arulrajah, A., Horpibulsuk, S., Anggraini, V., 2018. Practical
642 approach to predict the shear strength of fibre-reinforced clay. Geosynthetics International,
643 25(1): 50-66.
644 Mirzababaei, M., Mohamed, M., Miraftab, M., 2017. Analysis of strip footings on fiber-reinforced
645 slopes with the aid of particle image velocimetry. Journal of Materials in Civil Engineering,
646 29(4): 04016243.
647 Mohamed, M.H.A., 2010. Two dimensional experimental study for the behaviour of surface footings
648 on unreinforced and reinforced sand beds overlying soft pockets. Geotextiles and
649 Geomembranes, 28(6): 589-596.
650 Pomakhina, E., Deneele, D., Gaillot, A.-C., Paris, M., Ouvrard, G., 2012. 29Si solid state NMR
651 investigation of pozzolanic reaction occurring in lime-treated Ca-bentonite. Cement and
652 concrete research, 42(4): 626-632.
653 Puppala, A.J., Intharasombat, N., Vempati, R.K., 2005. Experimental Studies on Ettringite-Induced
654 Heaving in Soils. Journal of Geotechnical and Geoenvironmental Engineering, 131(3): 325-
655 337.
656 Rogers, C.D.F., Roff, T.E.J., 1997. Lime modification of clay soils for construction expediency.
657 Proceedings of the Institution of Civil Engineers - Geotechnical Engineering, 125(4): 242-249.
658 Singh, J., Huang, P.M., Hammer, U.T., Liaw, W.K., 1996. Influence of citric acid and glycine on the
659 adsorption of mercury (II) by kaolinite under various pH conditions. Clays and clay minerals,
660 44(1): 41-48.
661 Strawn, D.G., Bohn, H.L., O'Connor, G.A., 2015. Soil chemistry. John Wiley & Sons.
662 Vitale, E., Deneele, D., Paris, M., Russo, G., 2017. Multi-scale analysis and time evolution of
663 pozzolanic activity of lime treated clays. Applied Clay Science, 141: 36-45.
664 Vitale, E., Deneele, D., Russo, G., 2016. Multiscale Analysis on the Behaviour of a Lime Treated
665 Bentonite. Procedia Engineering, 158: 87-91.
666 Yaghoubi, M., Arulrajah, A., Disfani, M., Horpibulsuk S., Darmawan S., Wang J., 2019. Impact of
667 field conditions on the strength development of a geopolymer stabilized marine clay.
668 Applied Clay Science, 167: 33-42.
669 Zhao, H., Liu, J., Guo, J., Zhao, C., Gong, B.-w., 2015. Reexamination of Lime Stabilization Mechanisms
670 of Expansive Clay. Journal of Materials in Civil Engineering, 27(1).

671